

Confirmation of Arabia plate slow motion by new GPS data in Yemen

Christophe Vigny,¹ Philippe Huchon,^{1,2} Jean-Claude Ruegg,³ Khaled Khanbari,⁴
and Laike M. Asfaw⁵

Received 14 June 2004; revised 11 April 2005; accepted 31 October 2005; published 7 February 2006.

[1] During the last 10 years, a network of about 30 GPS sites was measured in Djibouti, East Africa. Additional points were also measured in Yemen, Oman, Ethiopia, Iran, and on La Réunion island. Merged with data from the available International GPS Service permanent stations scattered on the different plates in the area (Eurasia, Anatolia, Africa, Arabia, Somalia), this unique data set provides new insight on the current deformation in the Africa-Somalia-Arabia triple junction area and on the Arabian plate motion. Here we show that coherent motions of points in Yemen, Bahrain, Oman, and Iran allow us to estimate a geodetically constrained angular velocity for the Arabian plate (52.59°N , 15.74°W , $0.461^{\circ}/\text{Myr}$ in ITRF2000). This result differs significantly from earlier determinations and is based upon our vectors in Yemen. They provide new additional data and better geometry for angular velocity determination. Combined with the African and Somalian motions, this new angular velocity results in predicted spreading rates in the Red Sea and the Gulf of Aden which are 15–20% lower than those measured from oceanic magnetic anomalies and thus averaged over the last 3 Myr. With respect to Eurasia, the geodetic motion of Arabia is also about 30% slower than predicted by NUVEL-1A. On the basis of the kinematic results presented here and on other evidence for a similar slower geodetic rate of the Indian plate, we suggest that the whole collision zone between Africa, Arabia, India on one hand and Eurasia on the other hand has slowed down in the last 3 Myr.

Citation: Vigny, C., P. Huchon, J.-C. Ruegg, K. Khanbari, and L. M. Asfaw (2006), Confirmation of Arabia plate slow motion by new GPS data in Yemen, *J. Geophys. Res.*, *111*, B02402, doi:10.1029/2004JB003229.

1. Introduction

[2] A spectacular test of the plate rigidity hypothesis comes from the general agreement between the NUVEL-1A plate motion model [Argus and Gordon, 1991; DeMets *et al.*, 1994] and space geodetic measurements [Larson *et al.*, 1997]. This agreement also suggests that the present-day motions coincide with those averaged over the last 3 Myr. However, plate velocities are known to change through time, although the reason for that remains partly unclear. For example, the dramatic decrease in the relative velocity of India with respect to Eurasia has been attributed to the India-Eurasia collision at about 50 Ma [e.g., Patriat and Achache, 1984]. More subtly, the description of the Africa-Eurasia convergence also shows fluctuations [Dewey *et al.*, 1989; Rosenbaum *et al.*, 2002] that are often

more difficult to interpret. Part of these variations may be due to errors in the determination of kinematic parameters, but still it appears that at a given point, increase or decrease of the order of 5–20 mm/yr are predicted by plate kinematics. Therefore there is no a priori reason for present-day plate motions to be identical to those predicted by “geological” instantaneous model such as NUVEL-1A, which is based on measured velocities averaged over the last 3 Myr, in spite space geodetic measurements have often shown a fairly good agreement with NUVEL-1A [Larson *et al.*, 1997]. Given that plate motions obviously change over time, information on how fast and often these changes occur are important for addressing plate dynamics.

[3] On the basis of space geodetic measurements, McClusky *et al.* [2000] and Kreemer *et al.* [2003] first pointed out that Arabia is currently moving more slowly than predicted by NUVEL-1A. In their global kinematic model, Sella *et al.* [2002] also conclude that some plates, including Arabia and India, may move slower than predicted by NUVEL-1A. They found an angular velocity vector for Arabia (51.47°N , 2.89°E , $0.521^{\circ}/\text{Myr}$ in ITRF-97 reference frame), significantly different of the NNR-NUVEL-1A vector (45.20°N , 4.40°W , $0.545^{\circ}/\text{Myr}$). However, their determination for the Arabian plate is based on two geodetic sites only (one GPS in Bahrein and one satellite laser ranging (SLR) in Riyadh) and may thus be subject to discussion. An updated global model has been recently

¹Laboratoire de Géologie, Ecole Normale Supérieure, CNRS, Paris, France.

²Laboratoire de Tectonique, Université Pierre et Marie Curie, Paris, France.

³Laboratoire de Sismotectonique, Institut de Physique du Globe, CNRS, Paris, France.

⁴Department of Geosciences, University of Sana'a, Sana'a, Yemen.

⁵Addis Observatory, Department of Geophysics, Addis Ababa University, Addis Ababa, Ethiopia.

proposed by *Prawirodirjo and Bock* [2004] but unfortunately does not handle correctly the Arabia motion since it uses 5 stations which are very close to the Levant Fault or even on the western side of the fault, on the Sinai block, not on Arabia. The analysis of the same stations by *Wdowinski et al.* [2004] indeed shows they are within the zone of elastic strain accumulation. *McClusky et al.* [2003] addressed the question of the Arabia motion with four GPS sites, three of them (KIZI, GAZI, and KRCD) close to the Bitlis suture zone and East Anatolian Fault (EAF). Although they argue that the sites are far enough from the main faults to be outside the elastic strain field, using these stations is disputable because of the shortening that may occur farther south within the Arabian plate, in the Palmyride fold-and-thrust belt.

[4] A significant improvement of the kinematic constraints on the geodetic motion of Arabia comes from a regional survey performed in Iran and northern Oman [*Nilforoushan et al.*, 2003; *Vernant et al.*, 2004]. Among the 27 GPS sites measured, three (KHAS, KHOS, and MUSC) are well within the Arabia plate, away enough from the plate boundary, and were used by *Vernant et al.* [2004], together with BHR and the three stations of *McClusky et al.* [2003] mentioned above, to derive parameters of rotation for Arabia. We shall discuss their results in comparison with those presented in this paper, in which we use an improved and larger data set, including four new sites in Yemen and several sites in Djibouti and Ethiopia, to assess the motion of Arabia with respect to neighboring plates.

2. GPS Data Set and Processing

[5] In November 1991 the first observations of a 30-point GPS network were made in the junction zone of the Somalian, Arabian and African plates around the Afar region [*Ruegg et al.*, 1993; *Walpersdorf et al.*, 1999]. During the following decade, many of those points were remeasured periodically, including a remeasurement of four points in Yemen in 2001. Campaigns conducted in the framework of a French-Iranian program provide data on points located in Oman and southern Iran in 1999 and 2001 [*Nilforoushan et al.*, 2003; *Vernant et al.*, 2004]. Data from the 12 Iranian sites of the Asia-Pacific Regional Geodetic Project (APRGP) (1997–2001) are included. Occasional measurement on La Réunion island were also used. As many as 42 stations from the International GPS Service for Geodynamics (IGS) network [*Neilan*, 1995], spanning six plates (Eurasia, Anatolia, India, Africa, Somalia, and Arabia), are included in the processing. This not only allows improvement in the spatial coverage where campaign data are scarce but also allows “tie” in of the different networks to each other. The actual number of stations used in each campaign analysis is shown in Table 1.

[6] We analyze our GPS observations with the GAMIT/GLOBK software [*King and Bock*, 2000; *Herring*, 1999]. Twenty-four hour measurement sessions are reduced to daily positions using the LC Ionosphere free combination and fixing the ambiguities to integer values when possible. We used precise orbits from the IGS [*Beutler et al.*, 1993], except for the 1991 and 1993 campaigns for which we adjusted global orbits provided by Scripps Institution of

Oceanography (SIO). We also used IGS tables for modeling of antenna phase center variations. We do not use externally determined meteorological data but rather use the data themselves to estimate tropospheric delay parameters (once every 3 hours). More detailed explanations concerning the older data set processing (1991 to 1995) can be found in *Walpersdorf et al.* [1999]. For most regional-scale baselines, length repeatabilities (i.e., root-mean-square dispersion of baselines length about their mean value) steadily improve from around 10 mm in 1991, to standard values of around 1 to 3 mm since 1997.

[7] Solutions in a consistent reference frame were obtained at all epochs by including data from as many IGS permanent stations available around our study area at the time of the campaigns. This list increased from the small number of 4 stations in 1991 to 42 in 2003 and include 16 stations in Europe and central Asia (BRUS, GRAZ, JOZE, KIT3, MADR, MATE, METS, NOTO, ONSA, POL2, POLV, SOFI, USUD, WSRT, WTZR, ZECK), 12 stations in and around Africa (GOUG, HARK, LAMP, MALI, MAS1, MBAR, MSKU, NKLG, RABT, SUTH, TGCV, YKRO), 9 stations in the Middle East (AMMN, ANKR, BHR, DRAG, DYR2, NICO, Nssp, RAMO, TRAB), and 5 stations spread in the Indian Ocean (DGAR, IISC, MALD, REUN, SEY1). These daily data were combined with the daily global GAMIT solutions from SCRIPPS IGS center (including more than 200 stations spread all over the world) into a loose system using Helmert-type transformations in which translation, rotation, scale and Earth orientation parameters (polar motion and rotation) are estimated. The reference frame is then defined by minimizing, in the least squares sense, the departure from a priori values based on the International Terrestrial Reference Frame (ITRF) 2000 [*Altamimi et al.*, 2002], of the positions and velocities of a set of 22 well-determined stations in and around our study area (Ankara (ANKR), Ekaterinburg (ARTU), Bahrein (BHR), Bruxelles (BRUS), DiegoGarcia (DGAR), Kiev (GLSV), Gough Island (GOUG), Graz (GRAZ), Hartebeesthoek (HARK), Bangalore (IISC), Jozefoslaw (JOZE), Kittab (KIT3), Malindi (MALI), MasPalomas (MAS1), Matera (MATE), Metsohavi (METS), Onsala (ONSA), Bishkek (POL2), Mitzpe Ramon (RAMO), Sutherland (SUTH), Westerboork (WSRT), and Wetzell (WTZR)). The total misfit to those fiducial stations is 2.8 mm for positions (after rejection of IISC and MALI) and 1.6 mm/yr for velocities. Such small values indicate that local velocities are consistently computed in a stable reference frame.

[8] It has long been recognized that without adding a proper noise model to GPS data processing, we obtain unrealistic very low uncertainties on rates determined over long periods of time. In other words, because we use many epochs the straight line which fits station positions at different epochs is determined with a very low uncertainty, but very commonly does not intersect these epoch positions with their formal uncertainties. This does not mean that the rate inferred from the time series is in error, but that its uncertainty is not correct. When using continuous measurements and daily time series, robust mathematical models of different kinds of noise (white noise, random walk noise, flicker noise) can be tested and applied to the data (for a complete discussion, see, e.g., *Williams et al.*

Table 1. Data Set Used for This Study^a

Site	Station																				
	A91	A93-1	A93-2	A93-3	R95	A95	A97	I97	R97	I98	A99	O99	I99	R99	A00	I00	A01	O01	R02	I02	A03
BRUS	-	-	-	-	x	x	x	x	x	x	x	x	x	x	x	x	x	x	x	x	x
GRAZ	-	x	x	x	x	x	-	x	x	x	x	x	x	x	-	x	-	x	x	x	-
MADR	x	x	x	x	x	x	x	x	x	x	-	-	-	-	-	-	x	x	x	x	x
MATE	-	x	x	x	x	x	x	x	x	x	x	x	x	x	x	x	x	x	x	x	x
METS	-	x	x	x	x	-	-	x	x	x	-	x	x	x	x	x	x	x	x	x	x
NOTO	-	-	-	-	-	-	-	x	-	x	-	x	x	x	-	-	-	x	-	x	-
ONSA	x	x	x	x	x	x	x	x	x	x	x	x	x	x	x	x	x	x	x	x	x
SOFI	-	-	-	-	-	-	-	x	x	x	-	x	x	x	-	x	x	x	x	x	x
WSRT	-	-	-	-	-	-	-	x	x	x	x	x	x	x	x	x	x	x	x	x	x
WTZR	x	x	x	x	-	x	x	x	x	x	x	x	x	x	x	x	x	x	x	x	x
ARTU	-	-	-	-	-	-	-	-	-	-	-	x	x	x	x	x	x	x	x	x	x
GLSV	-	-	-	-	-	-	-	-	-	x	x	x	x	x	x	x	x	x	x	x	x
JOZE	-	-	-	x	x	-	-	x	x	x	-	x	x	x	-	x	x	x	x	x	x
KIT3	-	-	-	-	x	x	x	x	x	x	-	x	-	-	-	x	x	x	-	-	x
POL2	-	-	-	-	-	-	x	x	x	x	x	x	x	x	x	x	x	x	-	x	x
USUD	-	x	x	x	x	x	x	x	x	x	x	x	x	x	x	-	x	x	x	x	x
ZECK	-	-	-	-	-	-	-	x	x	x	-	x	x	x	-	x	x	x	x	x	x
ADD1	x	-	-	-	-	x	x	-	-	-	x	-	-	-	-	-	x	-	-	-	x
GOUG	-	-	-	-	-	-	-	-	-	x	x	x	x	x	x	x	x	x	x	x	x
HARK	-	-	-	-	-	-	-	-	x	x	x	x	x	x	x	x	x	x	x	x	x
LAMP	-	-	-	-	-	-	-	-	-	-	-	x	x	x	-	x	-	x	x	x	x
MAS1	-	x	x	x	x	x	x	x	x	x	x	x	x	x	x	x	x	x	x	x	x
MBAR	-	-	-	-	-	-	-	-	-	-	-	-	-	-	-	-	-	x	-	-	-
MSKU	-	-	-	-	-	-	-	-	-	-	-	-	-	-	-	-	-	x	x	-	-
NKLG	-	-	-	-	-	-	-	-	-	-	-	-	-	-	x	x	x	x	x	x	x
RABT	-	-	-	-	-	-	-	-	-	-	-	-	-	-	-	x	x	x	x	x	x
SUTH	-	-	-	-	-	-	-	-	-	x	x	x	x	x	x	x	x	x	x	x	x
YKRO	-	-	-	-	-	-	-	-	-	-	-	x	-	-	-	-	-	-	-	-	-
CBL0	x	-	-	-	-	x	-	-	-	-	x	-	-	-	-	-	-	x	-	-	x
GOR0	x	-	-	-	-	-	-	-	-	-	-	-	-	-	-	-	-	-	-	-	x
LLL0	x	-	-	x	-	x	x	-	-	-	x	-	-	-	-	-	x	-	-	-	x
MALI	-	-	-	-	-	-	x	x	x	x	x	x	x	x	x	x	-	x	x	x	x
REUN	-	-	-	-	-	-	-	-	-	-	-	-	-	x	-	-	-	x	x	x	x
SEY1	-	-	-	-	-	-	x	-	-	-	-	x	-	-	-	-	x	x	x	-	-
AMMN	-	-	-	-	-	-	-	-	-	-	-	x	x	x	-	x	-	x	x	-	-
BAHR	-	-	-	-	-	-	-	x	x	x	x	x	x	x	x	x	x	x	x	x	x
DHAM	x	-	-	-	-	-	-	-	-	-	-	-	-	-	-	-	x	-	-	-	-
HODD	x	-	-	-	-	-	-	-	-	-	-	-	-	-	-	-	x	-	-	-	-
JNAR	x	-	-	-	-	-	-	-	-	-	-	-	-	-	-	-	x	-	-	-	-
KHAS	-	-	-	-	-	-	-	-	-	-	-	x	-	-	-	-	-	x	-	-	-
KHOS	-	-	-	-	-	-	-	-	-	-	-	x	-	-	-	-	-	x	-	-	-
MUSC	-	-	-	-	-	-	-	-	-	-	-	x	-	-	-	-	-	x	-	-	-
SANA	x	x	x	x	-	x	-	-	-	-	x	-	-	-	-	-	x	-	-	-	-
DRAG	-	-	-	-	-	-	-	-	-	-	-	-	x	-	-	x	-	-	x	x	x
RSB0	x	-	-	-	-	-	-	-	-	-	x	-	-	-	-	-	x	-	-	-	x
RAMO	-	-	-	-	-	-	-	-	-	x	x	x	x	x	x	x	x	x	x	x	x
MALD	-	-	-	-	-	-	-	-	-	-	-	x	x	x	-	x	-	x	-	-	x
IISC	-	-	-	-	-	x	x	x	x	x	x	x	x	x	x	x	x	x	x	x	x
DGAR	-	-	-	-	-	-	x	x	x	x	x	x	x	x	x	x	x	-	-	x	x
ANKR	-	-	-	-	-	-	x	x	x	x	x	x	x	x	x	-	x	x	x	x	x
NICO	-	-	-	-	-	-	-	x	x	-	-	x	x	x	-	x	x	x	x	x	x
NSSP	-	-	-	-	-	-	-	-	-	x	-	-	-	-	-	-	-	x	-	x	-
TRAB	-	-	-	-	-	-	-	-	-	-	-	-	-	-	-	x	x	x	x	x	x
AHVA	-	-	-	-	-	-	-	-	-	-	-	-	-	-	-	x	-	x	-	-	-
LADA	-	-	-	-	-	-	-	x	-	x	-	-	x	-	-	x	-	-	-	-	-
MARI	-	-	-	-	-	-	-	x	-	x	-	-	x	-	-	-	-	-	-	-	-
MASH	-	-	-	-	-	-	-	-	-	-	-	-	x	-	-	x	-	x	-	-	-
MIAN	-	-	-	-	-	-	-	-	-	-	-	x	-	-	-	-	-	x	-	-	-
NILO	-	-	-	-	-	-	-	x	-	x	-	-	x	-	-	-	-	-	-	-	-
REIH	-	-	-	-	-	-	-	x	-	x	-	x	x	-	-	-	-	x	-	-	-
ROSE	-	-	-	-	-	-	-	x	-	x	-	-	x	-	-	x	-	x	-	-	-
SHIR	-	-	-	-	-	-	-	-	-	-	-	x	-	-	-	-	-	x	-	-	-
TEHN	-	-	-	-	-	-	-	-	-	-	-	-	-	-	-	x	-	x	-	-	-
YAS1	-	-	-	-	-	-	-	x	-	x	-	-	x	-	-	-	-	x	-	-	-
ZABO	-	-	-	-	-	-	-	-	-	-	-	-	x	-	-	x	-	x	-	-	-

^aCrosses indicate whether a given station is available at the date of the campaign: Afar (A), Oman (O), Reunion (R), Iran (I), followed by the year final two digits. The precise denomination and dates of the GPS campaigns are AFAR91, 1991.9152; AFAR93-1, 1993.0790; AFAR93-2, 1993.2711; AFAR93-3, 1993.9501; REUN95, 1995.0315; AFAR95, 1995.2479; AFAR97, 1997.1301; IRAN97, 1997.7959; REUN97, 1997.9192; IRAN98, 1998.9082; AFAR99, 1999.1466; OMAN99, 1999.7356; IRAN99, 1999.8562; REUN99, 1999.9164; AFAR00, 2000.5150; IRAN00, 2000.7882; AFAR01, 2001.2233; OMAN01, 2001.7959; REUN02, 2002.0534; IRAN02, 2002.7795; AFAR03, 2003.2342.

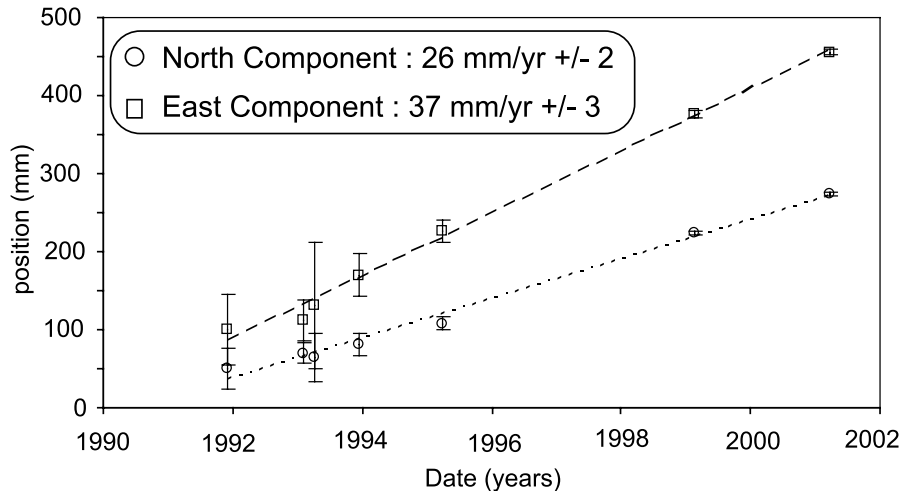


Figure 1. SANA time series in ITRF2000. North component (circles, short dashed lined), East component (squares, long dashed line). Error bars show the 3σ uncertainties.

[2004]). Unfortunately, for campaign like measurements it is an impossible task to infer the noise model from the data themselves and we have to use a priori assumption on the noise nature. One way of estimating realistic uncertainties is to simply rescale them (i.e., multiply them with and “ad hoc” factor). This factor can be determined as the ratio between the long-term noise (the difference between actual epoch positions and positions predicted using the linear fit) and the epoch formal uncertainty. A better way, more robust and better suited to GPS monuments behavior, is to consider that a time-dependent noise (i.e., random walk noise) is present in the determination of the stations position. In our processing, this is done by adding a moderate Markov noise ($2 \text{ mm}/\sqrt{\text{yr}}$) to the coordinates of stations when combining the daily solutions, following the procedures described by *Herring et al.* [1990] and *Herring* [1999]. Applying this strategy does not affect the velocity determination by more than 1 to 2 mm/yr but leads to the estimation of more realistic velocity uncertainties (1–2 mm/yr instead of the formal a priori value of 0.1 mm/yr). However, adding this noise to all stations would considerably alter the reference frame determination. Therefore we choose not to apply this noise model to the 22 global “reference” stations described earlier. Hence these stations still exhibit submillimeter uncertainties. When used to determine a pole rotation for a given plate, we multiply these velocity uncertainties by a factor of 10, to make them comparable to the average uncertainty of regional stations (1.3 mm/yr).

[9] As an example, Figure 1 depicts the time series (station position as a function of time) of our station in Sana’a, Yemen. This station was occupied 7 times between 1991 and 2001, and although the older measurements suffer from higher uncertainties and are affected by a less accurate realization of the reference frame, the velocity of this station is determined with a very small uncertainty (0.7 mm/yr on both horizontal components).

[10] Inversion of velocity data to obtain an angular velocity vector and associated uncertainties was performed by minimization of the weighted, L1 norm sum of misfits.

The choice of the L1 rather than L2 norm (or standard least squares) is justified by our wish to avoid too much emphasis on stations with large misfits (or “outliers”). Once an angular velocity is computed, we followed the procedure described by *Fernandes et al.* [2003] and checked that the obtained solution is stable with respect to the data set. First, we recompute the angular velocity vector with an unweighted scheme in order to check that the solution is not forced by the stations with the smaller uncertainties. Next, we checked that removing one or two of the stations does not change significantly the angular velocity vector.

3. Results

[11] Velocities in the ITRF2000 and relative to different plates are given in Table 2. Figures 2 and 3 depict large-scale velocities in a Eurasian reference frame (Figure 2) and an Arabian reference frame (Figure 3). Given the limited number (16) of Eurasian stations used in this study (most of which actually being in Europe) we choose not to estimate our own Eurasian reference frame but to use an external and well-determined Eurasia [*Calais et al.*, 2003]. Stations located in stable Eurasia exhibit very small residual velocities ($<1 \text{ mm/yr}$) in this reference frame, indicating that our solution is consistent with *Calais et al.* [2003]. However, stations in the most southern part of central Eurasia (ZECK, KIT3, POL2) show small but significant velocities relative to the rigid plate model. These velocities may be due to a slightly different rigid rotation pole, or may be representative of widespread deformation near these boundaries of the Eurasian plate [*Nocquet et al.*, 2001; *Wang et al.*, 2001; *Banerjee and Bürgmann*, 2002; *Sella et al.*, 2002].

3.1. Motion of Individual Plates

[12] The Africa (Nubia), Somalia, and Arabia plate motions are difficult to assess precisely given the small number of sites on these plates. Nevertheless, it is very clear that sites on the eastern side of the East African Rift and supposedly on the Somalia plate (MALI, SEY1, REUN) show a different block motion than sites on the western side

Table 2. Station Positions, Velocities in ITRF2000 and Relative to Eurasia, Africa, Somalia, and Arabia Plates and Uncertainties (1σ)^a

Site	Long	Lat	ITRF2000		Eurasia		Africa		Somalia		Arabia		σ		Corr
			Ve	Vn	Ve	Vn	Ve	Vn	Ve	Vn	Ve	Vn	dVe	dVn	
<i>Eurasia</i>															
BRUS	4.36	50.80	18.0	13.8	-0.4	-1.7	4.5	-4.9	-3.2	-10.1	14.9	3.1	0.05	0.03	0.022
GRAZ	15.49	47.07	21.8	14.2	0.6	0.1	4.6	-4.4	-3.8	-8.3	13.6	-2.0	0.06	0.04	-0.030
MADR	-4.25	40.43	18.9	15.6	0.1	-0.7	4.1	-2.7	-2.8	-8.8	7.7	9.4	0.63	0.61	-0.001
MATE	16.70	40.65	24.8	17.9	2.4	4.0	5.7	-0.7	-2.4	-4.4	11.0	1.2	0.05	0.03	0.005
METS	24.40	60.22	20.5	11.5	0.2	-1.0	4.6	-6.5	-4.3	-9.2	20.9	-8.6	0.05	0.04	-0.038
NOTO	14.99	36.88	21.5	18.1	-1.0	4.0	2.0	-0.5	-5.9	-4.4	5.0	2.2	0.91	0.90	0.000
ONSA	11.93	57.40	17.2	13.5	-1.2	-1.1	3.9	-5.2	-4.4	-9.5	18.5	-1.0	0.04	0.03	-0.045
SOFI	23.40	42.56	24.7	11.6	1.5	-1.1	4.6	-6.5	-3.9	-9.4	11.0	-8.1	0.86	0.85	0.000
WSRT	6.61	52.92	18.3	15.3	0.0	0.0	5.0	-3.5	-2.9	-8.4	16.7	3.4	0.06	0.04	-0.019
WTZR	12.88	49.14	20.9	14.4	0.5	-0.1	4.8	-4.3	-3.5	-8.5	14.9	-0.5	0.05	0.03	-0.003
ARTU	58.56	56.43	23.8	4.0	-1.5	-0.2	-0.8	-8.0	-9.9	-5.9	8.3	-26.0	0.38	0.27	-0.023
GLSV	30.50	50.36	20.9	12.2	-2.3	1.0	0.9	-5.1	-8.1	-7.0	11.6	-10.3	1.00	0.98	0.001
JOZE	21.03	52.10	22.0	12.9	0.6	-0.2	4.7	-5.4	-4.0	-8.5	16.7	-5.7	0.06	0.04	0.016
KIT3	66.89	39.14	30.9	3.2	3.8	1.4	3.2	-6.5	-5.1	-3.3	1.9	-27.7	0.07	0.04	-0.012
POL2	74.69	42.68	26.2	3.0	-0.9	3.4	-2.2	-4.5	-10.2	-0.3	-3.9	-28.2	0.08	0.04	-0.044
USUD	138.36	36.13	-4.2	-9.2	-25.7	6.0	-31.0	3.0	-34.2	11.1	-53.6	-22.8	0.71	0.67	-0.015
ZECK	41.57	43.79	25.9	10.5	0.5	1.8	2.3	-5.1	-6.6	-5.4	8.1	-15.7	0.87	0.85	0.000
<i>Africa</i>															
ADD1	38.77	9.04	25.3	16.5	1.8	7.1	1.3	0.4	-4.4	-0.3	-12.1	-8.9	0.70	0.65	0.002
GOUG	-9.88	-40.35	22.7	18.4	7.6	1.8	1.7	0.5	1.4	-6.0	-28.4	15.2	0.16	0.09	-0.219
HARK	27.71	-25.89	17.2	18.0	2.9	6.1	-0.5	0.3	-1.1	-1.9	-29.3	-3.5	0.09	0.05	0.077
LAMP	12.61	35.50	19.9	18.3	-2.4	3.8	0.5	-0.4	-7.2	-4.6	2.7	3.5	1.11	1.07	-0.002
MAS1	-15.63	27.76	16.6	17.2	-2.7	0.5	0.0	0.0	-6.0	-7.0	-4.9	17.1	0.06	0.03	0.045
NKLG	9.67	0.35	17.1	23.6	-4.5	8.7	-5.6	4.8	-10.2	0.3	-23.5	10.2	1.30	1.23	-0.004
MSKU	13.55	-1.63	34.6	28.8	13.3	14.4	12.0	10.1	7.7	6.0	-6.8	13.5	6.43	3.66	0.050
RABT	-6.85	34.00	14.4	16.1	-5.1	-0.3	-1.8	-2.1	-8.4	-8.4	-2.2	11.3	1.35	1.28	-0.005
SUTH	20.81	-32.38	15.7	18.7	3.0	5.5	-1.3	0.4	-1.1	-2.8	-32.1	0.1	0.10	0.06	0.003
<i>Somalia</i>															
CBL0	43.07	11.46	29.4	16.1	5.5	7.8	5.0	0.7	-1.0	0.6	-7.3	-10.6	0.69	0.63	0.001
GOR0	42.22	11.31	31.1	16.1	7.1	7.6	6.7	0.6	0.7	0.4	-5.6	-10.3	0.88	0.67	0.002
LLL0	42.58	11.26	30.3	15.6	6.4	7.1	6.0	0.1	0.0	0.0	-6.4	-10.9	0.68	0.63	-0.002
MALI	40.19	-3.00	26.5	14.2	5.7	5.1	4.3	-1.7	0.3	-2.2	-15.1	-11.6	0.14	0.05	-0.018
REUN	55.57	-21.21	17.6	10.6	3.2	5.6	1.4	-2.1	0.1	-0.4	-24.0	-18.9	1.31	1.13	0.009
SEY1	55.48	-4.67	21.2	9.1	1.0	4.1	-0.4	-3.6	-4.2	-1.9	-20.3	-20.4	1.36	1.05	0.028
<i>Arabia</i>															
AMMN	35.88	32.03	20.8	17.5	-4.5	7.5	-3.1	0.9	-11.2	-0.2	-3.4	-6.9	1.34	1.30	0.000
BAHR	50.61	26.21	31.6	28.6	5.4	22.3	5.6	14.8	-2.1	15.8	0.6	0.1	0.07	0.03	0.023
DHAM	44.39	14.58	35.6	28.0	11.1	20.0	10.8	12.9	4.4	13.0	0.1	1.0	0.83	0.73	-0.016
HODD	42.97	14.79	35.3	26.8	10.8	18.5	10.6	11.5	4.2	11.4	0.1	0.2	1.03	0.76	-0.053
JNAR	43.44	13.32	37.2	26.7	12.9	18.5	12.6	11.5	6.3	11.4	1.2	0.0	1.29	0.83	-0.067
KHAS	56.23	26.21	30.3	29.1	3.9	24.2	3.7	16.6	-3.8	18.3	-2.0	-0.6	1.50	1.40	-0.001
KHOS	48.41	30.25	27.2	24.5	0.9	17.6	1.4	10.2	-6.6	10.9	-1.2	-3.5	1.60	1.45	-0.002
MUSC	58.57	23.56	33.9	29.9	7.7	25.7	7.3	18.0	0.0	20.1	-0.1	-0.1	1.44	1.40	-0.002
REIH	51.08	28.92	27.2	29.5	0.8	23.2	1.1	15.8	-6.8	16.8	-2.6	0.8	1.02	1.00	-0.001
SANA	44.19	15.35	37.0	26.5	12.3	18.5	12.1	11.4	5.6	11.4	1.8	-0.5	0.77	0.72	-0.013
DRAG	35.39	31.59	24.4	19.3	-0.9	9.2	0.5	2.7	-7.6	1.5	0.0	-4.9	1.14	1.09	0.004
RAMO	34.76	30.60	17.7	15.8	-7.5	5.5	-6.2	-1.0	-14.2	-2.2	-7.3	-8.3	0.10	0.04	0.022
RSB0	43.36	11.98	36.7	24.6	12.6	16.4	12.2	9.3	6.1	9.3	0.2	-2.1	1.21	1.01	-0.010
<i>India</i>															
DGAR	72.37	-7.27	46.4	31.2	27.1	31.0	26.0	23.1	22.4	27.0	5.9	0.1	0.18	0.07	0.128
IISC	77.57	13.02	37.4	32.9	12.7	34.2	11.3	26.4	5.4	30.9	-2.7	1.8	0.10	0.04	-0.036
MALD	73.53	4.19	36.4	42.5	13.7	42.6	12.5	34.7	7.5	38.8	-4.2	11.3	1.10	1.06	0.001
<i>Anatolia</i>															
ANKR	32.76	39.89	-2.2	13.1	-26.9	2.4	-24.7	-3.9	-33.3	-5.4	-20.3	-10.2	0.07	0.03	0.038
NICO	33.40	35.14	19.2	14.6	-5.8	4.0	-4.0	-2.3	-12.3	-3.8	-2.4	-8.9	0.86	0.85	0.001
NSSP	44.50	40.23	28.8	15.2	2.9	7.2	4.3	0.1	-4.4	0.2	7.7	-11.9	0.97	0.96	0.001
TRAB	39.78	41.00	24.8	11.1	-0.6	2.0	1.2	-4.8	-7.5	-5.4	5.7	-14.6	1.30	1.26	0.003
<i>Iran</i>															
AHVA	48.68	31.34	27.3	23.4	1.0	16.5	1.5	9.2	-6.6	9.9	-0.5	-4.7	2.19	2.04	0.005
LADA	55.90	28.29	29.1	24.9	2.5	20.0	2.5	12.4	-5.3	14.1	-2.1	-4.6	1.20	1.16	-0.003
MASH	59.47	36.31	24.9	6.3	-2.1	2.4	-2.1	-5.4	-10.4	-3.2	-3.2	-23.8	1.51	1.45	-0.003
MIAN	46.16	36.91	25.9	21.1	-0.3	13.6	0.8	6.3	-7.8	6.7	2.1	-6.4	1.50	1.41	0.000
MARI	51.81	35.73	27.8	17.2	1.2	11.2	1.8	3.7	-6.6	4.9	1.7	-11.5	1.46	1.40	-0.004
NILO	48.34	32.42	20.2	25.6	-6.2	18.6	-5.5	11.3	-13.7	11.9	-6.9	-2.5	1.46	1.40	-0.002
ROSE	53.82	32.31	23.6	19.8	-3.0	14.3	-2.8	6.7	-10.9	8.2	-5.0	-9.4	1.02	1.00	0.000

Table 2. (continued)

Site	Long	Lat	ITRF2000		Eurasia		Africa		Somalia		Arabia		σ		Corr
			Ve	Vn	Ve	Vn	Ve	Vn	Ve	Vn	Ve	Vn	dVe	dVn	
SHIR	57.31	37.81	26.0	9.8	-0.9	5.3	-0.7	-2.5	-9.1	-0.5	-0.6	-20.0	1.48	1.40	0.000
TEHN	51.33	35.70	32.4	16.5	5.8	10.4	6.4	2.9	-2.0	4.0	6.4	-12.1	2.16	2.03	0.001
YAS1	58.46	35.29	31.2	12.3	4.3	8.1	4.3	0.4	-4.0	2.5	2.8	-17.7	1.03	1.00	-0.001
ZABO	61.52	31.05	29.7	6.7	2.8	3.4	2.4	-4.5	-5.5	-2.0	14.9	3.1	1.52	1.45	-0.003

^aBold numbers highlight stations velocity residuals with respect to the plate that they belong to. Station names in bold indicate stations used for the mapping in ITRF2000. Long, longitude; Lat, latitude; Corr, correlation.

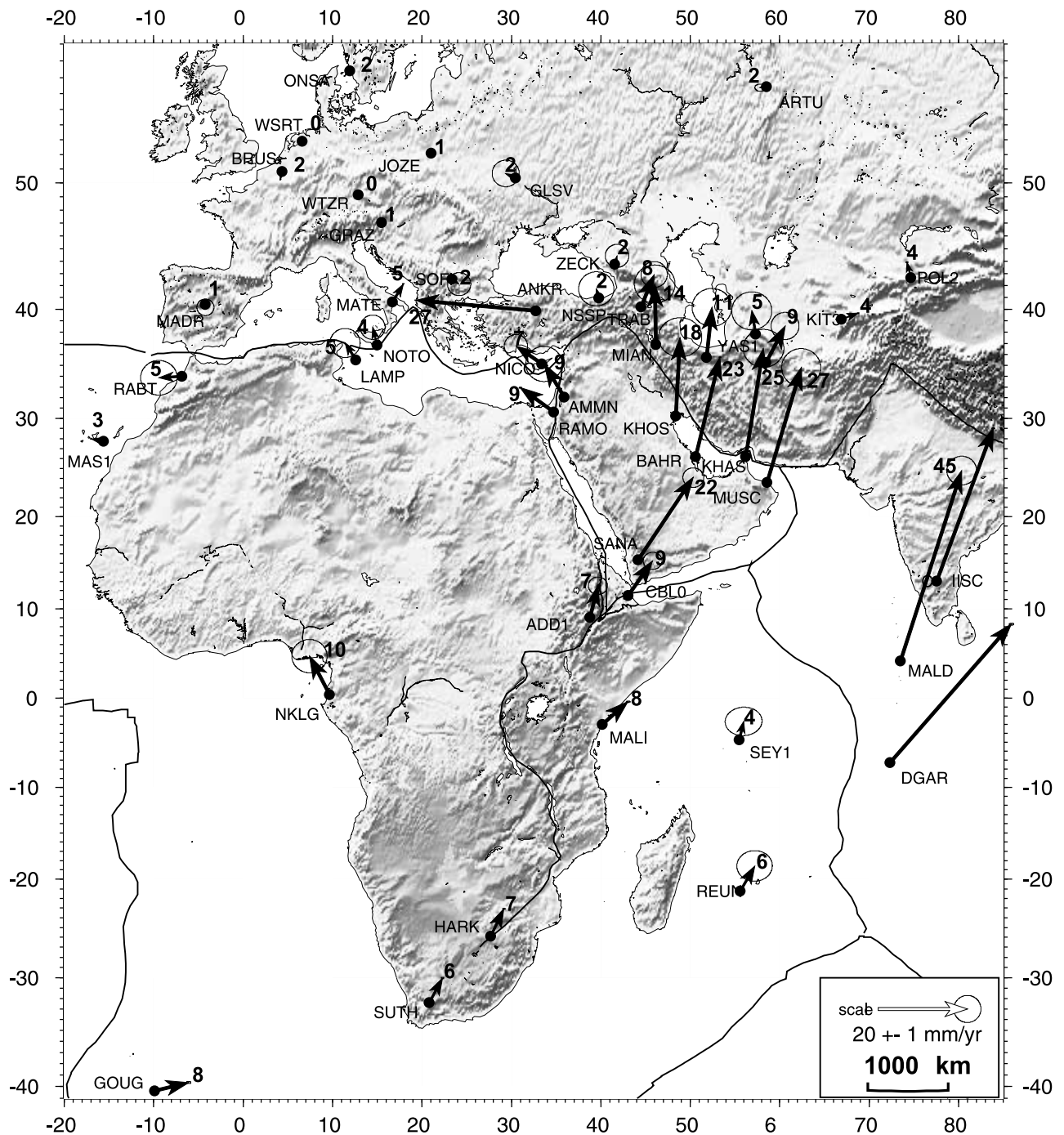


Figure 2. Large-scale velocities in the ITRF2000 reference frame, relative to Eurasia as defined by Calais et al. [2003]. Ellipses show the 99% confidence level of the a priori formal uncertainties given in Table 2. Numbers next to arrow heads indicate the station velocity in mm/yr.

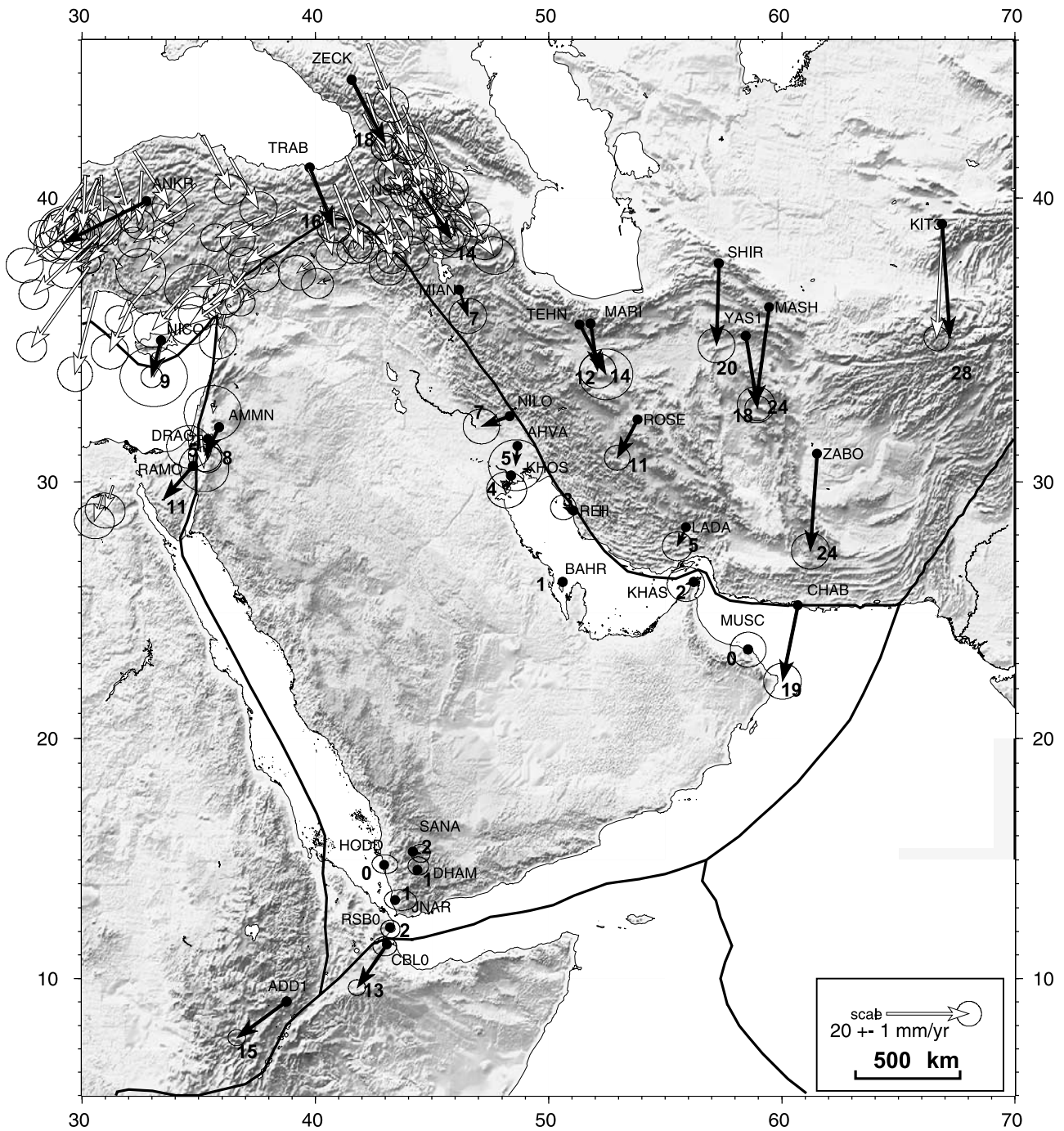


Figure 3. Arabian sites velocities in the ITRF2000 reference frame, relative to Arabia defined in this work. Solid arrows depict our solution; open arrows are for *McClusky et al.* [2000]. For our solution, ellipses show the 99% confidence level of the velocity uncertainties given in Table 2. Numbers next to arrow heads indicate the station velocity in mm/yr.

of the East African Rift (MAS1, RABT, LAMP, NKLG, GOUG) and supposedly on stable Africa. Some sites located closer to the East African Rift have needed closer inspection to determine whether they belong to Africa or Somalia, but the result was generally unambiguous: for instance, although HART and SUTH are located close to the plate boundary, their motion is better fit with Africa than with Somalia (although the difference is small), in agreement with their location to the west of the East African Rift.

3.1.1. Africa

[13] *Sella et al.* [2002] used five sites on the African plate (GOUG, HART, HRAO, MASP, and SUTH), two of them being very close (HRAO and HART) making their solution actually constrained by only four sites. *Fernandes et al.* [2003] used a larger data set of ten stations, including five IGS stations (MAS1, HRAO, SUTH, GOUG, and NKLG). In addition to MAS1, SUTH, GOUG, and NKLG (we did not use HRAO because no data was available during the

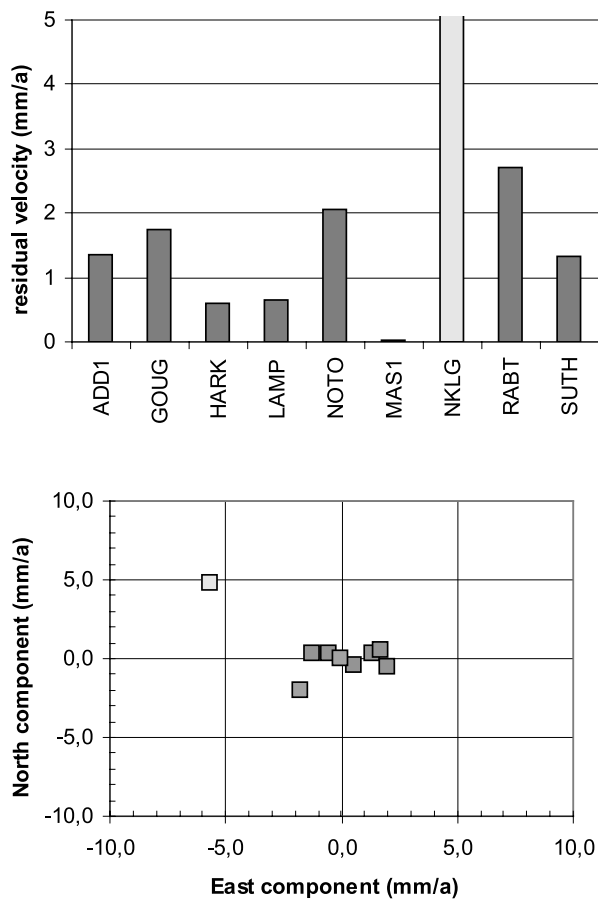


Figure 4. African plate stations residual velocities with respect to our determination of the African plate motion. (top) Velocity magnitudes and (bottom) velocity components in mm/yr. Light shaded symbols depict stations with high-velocity uncertainties or lying in deformation zones (usually not used in the pole determination).

campaigns), we used five additional sites in our analysis: HARK (that replaced HART), RABT, LAMP, and NOTO in North Africa and Sicily) and ADD1 (the site in Addis Ababa that belongs to our regional network). In spite of the small number (9) of sites, the African plate is spatially reasonably well covered. We computed an angular velocity vector (50.48°N , 82.01°W , $0.265^\circ/\text{Myr}$) with respect to ITRF2000 (Table 3), not significantly different from that of *Fernandes et al.* [2003] at the 1σ level. It differs from

that of *Sella et al.* [2002], but the reference frame (ITRF97) is also different. Note that since *Calais et al.* [2003] do not give the parameters of rotation for Africa with respect to ITRF2000, we computed them from their Africa-Eurasia solution and from the Eurasia motion in ITRF2000 with an angular velocity vector (52.3°N , 107.0°W , $0.245^\circ/\text{Myr}$) (E. Calais, personal communication, 2004). Figure 4 shows the individual misfits at the nine sites we used. The RMS residual is 0.9 mm/yr , and the misfit at all stations is less than 2 mm/yr except for RABT and NKLG. These two stations, however, may not be reliable. The north component of the velocity at RABT indeed shows oscillations and the time series is noisy, and the velocities at NKLG provided by various processing centers are surprisingly very different, suggesting some technical problems. However, we kept these two stations because removing them does not change significantly the solution (50.43°N , 82.96°E , $0.266^\circ/\text{Myr}$). We also recomputed the angular velocity vector with an unweighted procedure and found a very small difference (0.2° in latitude, 0.3° in longitude, same rate). Finally, we concur with *McClusky et al.* [2003] and *Fernandes et al.* [2003] that the geodetic African motion, in spite of the relatively small number of stations and the use of stations close to plate boundary which velocity could be affected by deformation (e.g., NOTO or HARK), is now reasonably well constrained.

3.1.2. Somalia

[14] The motion of Somalia is constrained by even fewer data than Africa: only two sites (MALI and SEY1) were used by *Sella et al.* [2002], making the determination of the pole unambiguous but not well constrained. *Fernandes et al.* [2003] used four sites (MALI, SEY1, REUN, and RBAY). We did not use RBAY in our computations because no data were available during the various campaigns, but we added three sites of the Djibouti regional network which are clearly outside the deforming zone: CBL0, LLL0, and GOR0 (C. Vigny et al., 12 years of geodetic measurements in the Asal Rift, Djibouti, submitted to *Journal of Geophysical Research*, 2004). Inversion of the velocities at these six sites leads to an angular velocity vector (47.69°N , 98.32°W , $0.330^\circ/\text{Myr}$). In spite of a poor fit at SEY1 (4 mm/yr), the RMS residual on the six velocities is 0.8 mm/yr (Figure 5). We checked the stability of our solution in the same way as for Africa. The unweighted inversion leads to nearly the same angular velocity vector (only the latitude differs by 0.04°), but removing SEY1, for which the time series shows numerous gaps, slightly changes the solution (48.12°N , 97.75°W , $0.329^\circ/\text{Myr}$)

Table 3. Rotation Parameters of Africa, Somalia, Arabia, and India With Respect to ITRF2000^a

Plate	Lat, °N	Long, °E	Rate °/Myr	σ Rate °/Myr	σ maj, deg	σ min, deg	azim, deg	Reference
AFR	50.48	-82.01	0.265	0.003	1.26	0.74	276	this work
AFR	46.64	-86.32	0.251					<i>Calais et al.</i> [2003]
AFR	50.86	-81.47	0.261	0.002	1.03	0.60	95	<i>Fernandes et al.</i> [2003]
AFR	52.25	-80.18	0.253	0.004	1.6	0.9	277	<i>Sella et al.</i> [2002]
SOM	48.12	-97.75	0.329	0.008	4.36	0.70	316	this work
SOM	54.63	-93.61	0.315	0.007	2.30	0.73	54	<i>Fernandes et al.</i> [2003]
SOM	53.51	-101.55	0.310	0.002	0.9	0.1	42	<i>Sella et al.</i> [2002]
ARA	52.59	-15.74	0.461	0.011	2.98	0.42	81	this work
ARA	51.47	2.89	0.521	0.024	3.1	0.7	290	<i>Sella et al.</i> [2002]
IND	50.90	-12.13	0.487	0.010	5.11	0.61	288	A. Socquet et al. (unpublished manuscript, 2004)

^aAFR, Africa; SOM, Somalia; ARA, Arabia; and IND, India. ITRF-97 for *Sella et al.* [2002]. Uncertainty on the pole location is given by the semimajor (σ maj) and semiminor (σ min) axes of the 1σ error ellipse (azim is the azimuth of the semimajor axis).

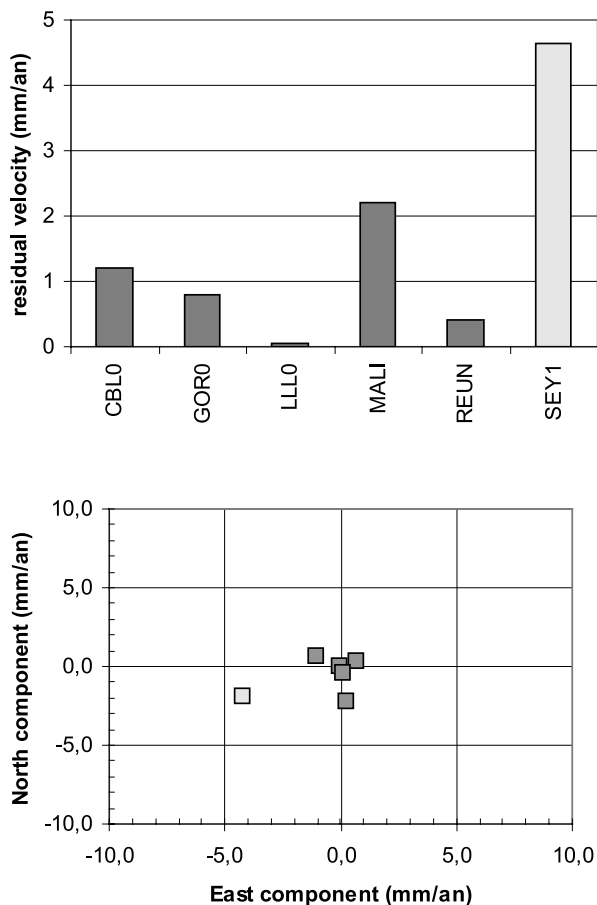


Figure 5. Somalian plate stations residual velocities with respect to our determination of the Somalian plate motion. (top) Velocity magnitudes and (bottom) velocity components in mm/yr. Light shaded symbols depict stations with high-velocity uncertainties or lying in deformation zones (usually not used in the pole determination).

(Table 3). Our solution for Somalia thus significantly differs from previous ones because it uses constraints in the northern part of the plate (sites CBL0, LLL0, and GOR0). *Sella et al.*'s [2002] and *Fernandes et al.*'s [2003] models show discrepancies of 2–4 mm/yr at these northern sites. At other sites (MALI, REUN, SEY1), the difference is small. Although the angular velocity vector is not as well constrained as the Africa one, we are thus fairly confident that our determination of the Somalia motion provides a better estimate than previously ones, a point that will be critical when dealing with relative motion around the Africa-Arabia-Somalia triple junction. Because it uses data in the northern part of the Somalia plate, our Somalian angular velocity vector provides a better estimate of the motion of Arabia with respect to the nearby part of Somalia, which was not the case with previous models.

3.1.3. Arabia

[15] In this work, the Arabia plate motion is constrained by a total of eleven sites: four stations in Yemen (DHAM, HODD, JNAR, and SANA), two in Oman (MUSC, KHAS), one in Bahrain (BAHR), two in Iran (KHOS, REIH), one in northern Djibouti, on the stable Danakil block (RSB0), and

one in Jordan (AMMN) (Figure 3). We did not use DRAG in our kinematic inversion because it shows elastic coupling with the Levant Fault. In terms of the number of sites and, even more important, spatial coverage, this is a significant improvement over previous models that used from only two [*Sella et al.*, 2002], four [*McClusky et al.*, 2003], and six [*Vernant et al.*, 2004]. Velocities of those 11 stations fit a rigid rotation about an angular velocity vector (52.26°N , 12.27°W , $0.470^\circ/\text{Myr}$). The RMS residual is 1.2 mm/yr, although one station (AMMN) shows a very large misfit (9 mm/yr). Although no technical problem has been reported, the time series available show that the north component of the velocity does not fit a straight line. Discarding this station gives an angular velocity vector (52.59°N , 15.74°W , $0.461^\circ/\text{Myr}$) (Table 3), thus more to the west at nearly the same latitude and accordingly a smaller rate. As for Africa and Somalia, we checked that our solution is stable with respect to the inversion scheme. Removing the two stations with misfits larger than 2 mm/yr (KHOS and REIH) slightly displaces the pole of rotation toward the west (by about 2°) and reduces accordingly the angular rate, but in the same way as for the two poorly fit African stations (RABT and NKLG), we decided to keep these two stations in our solution. Two other stations may pose problem: KHAS in Oman is extremely close to the boundary in the straights of Hormuz, and RSB0 in Djibouti on the Danakil block is within the Afar triple junction. Their velocity could be affected by elastic effects due to coupling with plate boundaries (KHAS) or distributed strain in a complex ridge-ridge-ridge triple junction (RSB0). However, rejecting them (which was done in a first estimation) does not change the determination of the plate angular velocity. Thus it is an a posteriori conclusion that despite their proximity with plate boundaries, these stations velocities are in fact not affected by deformation, or, if they are, it is small enough and affecting a sufficiently small number of points (2 out of 11) so that it does not affect the determination of the plate motion. The rotation parameters that we computed significantly differ from those determined by *Sella et al.* [2002]. Unfortunately, *McClusky et al.* [2003] and *Vernant et al.* [2004] do not provide their velocities and rotation parameters in ITRF, so that we cannot make a direct comparison with our solution. When compared with our measurements in Yemen, the predictions of *Sella et al.*'s [2002] model show significant, 3–4 mm/yr discrepancies. Consequently, as in the case of the Somalia plate, adding new sites where data were not previously available does change the rotation parameters, even if the predicted motion on previously existing sites is not significantly modified. In other words, we find a different rotation pole than previous studies because of new vectors in Yemen, but this different pole still predicts the same velocities than those previous studies at common stations (in particular in Oman). Therefore these previous studies are not erroneous (decimating our data we obtain the same results) but simply lack data in the southwestern “corner” of the plate. With the exception of AMMN and, to a less extend of KHOS and REIH, the residual velocities are small at all sites (<2 mm/yr) and show no systematic trend (Figure 6). Even at KHOS and REIH, the misfit does not exceed the 2σ uncertainty. We thus consider that these residual velocities represent the noise of our solution and therefore demonstrate the rigidity of the

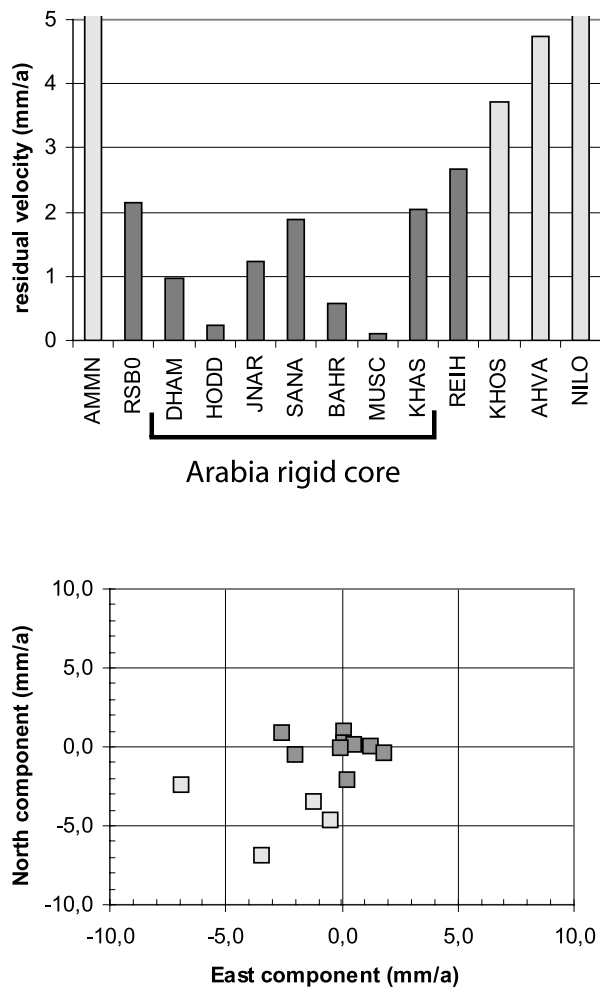


Figure 6. Arabian plate stations residual velocities with respect to our determination of the Arabian plate motion. (top) Velocity magnitudes and (bottom) velocity components in mm/yr. Light shaded symbols depict stations with high-velocity uncertainties or lying in deformation zones (usually not used in the pole determination).

Arabian plate at this level of around 2 mm/yr, or less than 10^{-9} strain/yr.

3.2. Relative Plate Motions

[16] A first test of our results and their implications is to compare the predictions in terms of relative motion with observations. The relative rate shown by our data between ADD1 in Ethiopia (west of East African Rift) and AR00, CBL0, LLL0, and GOR0 in Djibouti (east of the East African Rift) is about 5 mm/yr, east-west trending, consistent with other estimates of the East African Rift separation rate. *Bilham et al.* [1999] used a combination of SLR and GPS data to derive a rate of 4.5 ± 1 mm/yr at $N108^\circ \pm 10^\circ E$ across the northern Ethiopian rift at the latitude of Addis Ababa, in good agreement with previous “geological” estimates of *Jestin et al.* [1994] (5 mm/yr at $N102^\circ E$) and *Chu and Gordon* [1999] (6 mm/yr at $N95^\circ E$). Combining our African and Somalian angular velocities gives a Somalia/Africa vector of relative motion at ($28.95^\circ S$, $43.70^\circ E$, $0.084^\circ/Myr$) which is only slightly east of *Chu*

and *Gordon's* [1999] “geological” solution but very different from that of *Fernandes et al.'s* [2003]. However, because of the close locations of the two African and Somalia vectors, their sum is very sensitive to small variations (either in pole location or in angular rate) and the result is quite erratic in the absence of further constraints (see a discussion of this effect in combining two nearby poles by *Jestin et al.* [1994]). This is well illustrated by the large uncertainties obtained in combining the two covariance matrixes (semiaxes of the 1σ error ellipse are 11° and 4°). Thus the only way to determine with confidence a Somalia-Africa pole would be to compare it with measurements, which unfortunately are still lacking in the central and southern parts of the East African Rift.

3.2.1. Arabia-Africa: Red Sea and Levant Fault

[17] Combining our African and Arabian rotations leads to an angular velocity vector ($31.64^\circ N$, $20.29^\circ E$, $0.308^\circ/Myr$) (Table 4). The RMS misfit on observed velocities is <1.2 mm/yr. Our pole is close in latitude and longitude (within 1σ , i.e., around 3°) to those of *Jestin et al.* [1994] and *Chu and Gordon* [1998], established from oceanic magnetic anomalies in the Red Sea. It differs more in longitude from both *McClusky et al.* [2003] and *Sella et al.* [2002] (5° and 9° , respectively, i.e., more than 2σ). However, it is our rate which differs more: we confirm that the geodetic angular rate of rotation is significantly smaller than the geological one ($0.308^\circ/Myr \pm 0.05$ at 3σ versus 0.400 to $0.418^\circ/Myr$, with a pole longitude, however, slightly more to east). *McClusky et al.* [2003] already suggested some reduction of this rate (with $0.37^\circ/Myr$) but did not consider this reduction to be significant because of their larger uncertainty of $0.04^\circ/Myr$. Compared to *Chu and Gordon's* [1998] estimates based on magnetic anomalies, the Red Sea spreading is reduced from 9 mm/yr in the northern part and 18 mm/yr in the southern one to 8 and 15 mm/yr, respectively, thus by $\sim 15\%$. The difference is clearly hardly significant but corroborates an actual decrease in the Red Sea spreading rate since 3 Ma (or less), as argued by *Calais et al.* [2003] for the Africa-Eurasia-North America relative motions. Meanwhile, our predicted azimuths (023 and 044 in northern and southern Red Sea, respectively) are slightly more northerly than those predicted by *Chu and Gordon* [1998] (026 and 047). Again, those very small differences of 3° in direction are not really significant. Anyhow, since there is no clear transform directions in the Red Sea, we cannot test those predictions. In conclusion, if inferred on Red Sea data only, one could still argue against the decrease in rates of plate motion. Taking their uncertainties into account, GPS and NUVEL-1A rates are almost indistinguishable there.

[18] Along the Levant (Dead Sea) Fault system, our predicted rate of 7 mm/yr is very close to both the 8 mm/yr predicted by *Chu and Gordon* [1998] and the 6 mm/yr given by *McClusky et al.* [2003] but twice the 4 mm/yr predicted by *Sella et al.* [2002]. All these estimates fit well with the 4 ± 2 mm/yr geological estimate of *Klinger et al.* [2000]. On the basis of three GPS stations and a locked fault model (because two GSP stations, KATZ and ELAT, are close to the fault), *Pe'eri et al.* [2002] infer a 2.6 ± 1.1 mm/yr north-south component of motion, which is therefore a minimum estimate. On the basis of a larger network of 11 stations, *Wdowinski et al.* [2004] obtained a

Table 4. Relative Motion Parameters of Arabia, Africa, Arabia, India, and Eurasia Based on GPS and Conventional Kinematic Data^a

Lat, °N	Long, °E	Rate, °/Myr	σ Rate, °/Myr	σ maj, Δ Lat	σ min, Δ Lon	azim, deg	Reference
<i>ARA-AFR</i>							
31.64	20.29	0.308	0.018	2.5	1.1	290	this work
30.50	25.70	0.370	0.04	1.0	2.3	-	<i>McClusky et al.</i> [2003]
31.26	29.55	0.400	0.030	1.8	1.3	275	<i>Sella et al.</i> [2002]
31.50	23.00	0.400	0.05	1.2	2.7	-	<i>Chu and Gordon</i> [1998]
32.59	23.70	0.418	-	-	-	-	<i>Jestin et al.</i> [1994]
<i>ARA-SOM</i>							
20.07	25.49	0.356	0.026	2.3	1.2	286	this work
21.06	28.62	0.441	0.029	1.8	1.0	55	<i>Sella et al.</i> [2002]
25.24	23.39	0.423	-	-	-	-	<i>Jestin et al.</i> [1994]
24.10	24.00	0.40	0.05	4.9	1.3	295	<i>DeMets et al.</i> [1994]
<i>ARA-EUR</i>							
28.27	12.12	0.364	0.017	2.5	0.66	276	this work and Calais (personal communication, 2004)
27.90	19.50	0.410	0.1	0.5	1.4	-	<i>Vernant et al.</i> [2004]
26.20	20.40	0.437	0.023	3.7	0.9	77	<i>Kreemer et al.</i> [2003]
27.40	18.40	0.400	0.04	1.0	2.5	-	<i>McClusky et al.</i> [2003]
26.22	22.87	0.427	0.029	2.1	1.1	76	<i>Sella et al.</i> [2002]
24.60	13.70	0.52	0.05	5.2	1.7	288	<i>DeMets et al.</i> [1994]
<i>ARA-IND</i>							
19.73	20.42	-0.035	0.025	65.2	11.5	285	this work and A. Socquet et al. (unpublished manuscript, 2004)
10.5	61.83	0.099	0.073	17.2	10.4	88	<i>Sella et al.</i> [2002]
3.0	91.5	-0.03	0.04	26.1	2.4	302	<i>DeMets et al.</i> [1994]

^aARA, Arabia; AFR, Africa; ARA, Arabia; IND, India; and EUR, Eurasia. Uncertainty on the pole location is given either by the semimajor (σ maj) and semiminor (σ min) axes of the 1σ error ellipse (azim is the azimuth of the semimajor axis) or by the uncertainty in latitude (Δ Lat) and longitude (Δ Lon). Note that the NUVEL-1 [*DeMets et al.*, 1994] solution for ARA-AFR is actually ARA-SOM (Africa being treated as a single plate and data coming from the Gulf of Aden alone).

current slip rate of 3.3 ± 0.4 mm/yr along the Levant Fault system. This, however, might not be directly comparable to our 7 mm/yr estimate since GPS data show a significant motion of the Sinai subplate with respect to Africa. *Wdowinski et al.* [2004] predict a 2.4 mm/yr velocity along azimuth 201° across the Suez rift, between Sinai and Africa. This azimuth is nearly the trend of the Levant Fault, which implies a total relative motion of 5.7 mm/yr between Arabia and Africa, in very good agreement with *McClusky et al.* (6 mm/yr) and our estimate (7 mm/yr).

3.2.2. Arabia-Somalia: Gulf of Aden

[19] A further test of a possible slowing down of the Arabia motion is to look at the Gulf of Aden. Combining our Somalia and Arabia motions relative to ITRF2000 gives an angular velocity vector (20.07° N, 25.49° E, 0.356° /Myr) (Table 4). This is significantly different compared with all previously proposed solutions. When the Arabian sites velocities are rotated with respect to (our) Somalia, our solution gives a RMS misfit of 1.5 mm/yr. With *Sella et al.*'s [2002] solution, the misfit is 3 mm/yr on average, but everywhere larger than 2 mm/yr.

[20] Geologically based models [*DeMets et al.*, 1994; *Jestin et al.*, 1994] do not fit the GPS data, showing much larger predicted rates as well as azimuths rotated clockwise. In Oman, predicted velocities are 22–23 mm/yr instead of 19–20 mm/yr measured. In Yemen, predicted and observed values are 16 and 13 mm/yr, respectively. Along the Gulf of Aden, observed spreading rates range from 16 to 22 mm/yr from west to east, while our geodetic model predicts 13 to 18 mm/yr, $\sim 20\%$ less. This 3 mm/yr difference between velocities derived from GPS and from magnetic anomalies is larger, although only slightly, than the uncertainties. Our measurements thus indicate a present-day spreading rate in

the Gulf of Aden reduced by about 15–20% with respect to the rate averaged over the last 3 Myr. In terms of directions, we have compared the predicted values on three well-defined transform faults (Maita-Al Khalb, Alula-Fartak, and Socotra) with their actual trends and found a 6 – 7° clockwise rotation. A similar, although larger (18°), clockwise rotation of the spreading direction has been suggested by *Tamsett and Searle* [1988] on the basis of small-scale morphology. However, the change has been dated approximately at 3.5 Ma. If this is correct, it should also have been recorded in the magnetic anomalies, which does not seem to be the case. More work is thus needed to try to date the time of this kinematic change, a 20% decrease in velocity and a small clockwise rotation.

3.2.3. Arabia-India: Owen Fracture Zone and Murray Ridge

[21] The Owen fracture zone is a slowly slipping transform fault that accommodates right-lateral motion between the Indian and Arabian plates. Farther north and before it reaches the Pakistan triple junction the plate boundary in the vicinity of the Murray ridge is made of transform segments that strike parallel to the Owen fracture zone. Using slip vector azimuth data from *Quittmeyer and Kafka* [1984], NNR-NUVEL-1A constrained the relative motion between the two plates to a small 2 mm/yr right-lateral strike-slip motion with an azimuth ranging from $N20^\circ$ E in the south to $N40^\circ$ E in the north. Because it comes from present-day seismicity, this motion should match instantaneous rates inferred from geodesy on the last decade. In other words, any revision of the Arabia plate motion should be accompanied by a similar revision of the India plate motion, in order to preserve their close to zero relative motion. Recent geodetic determinations confirm a slower Indian rotation

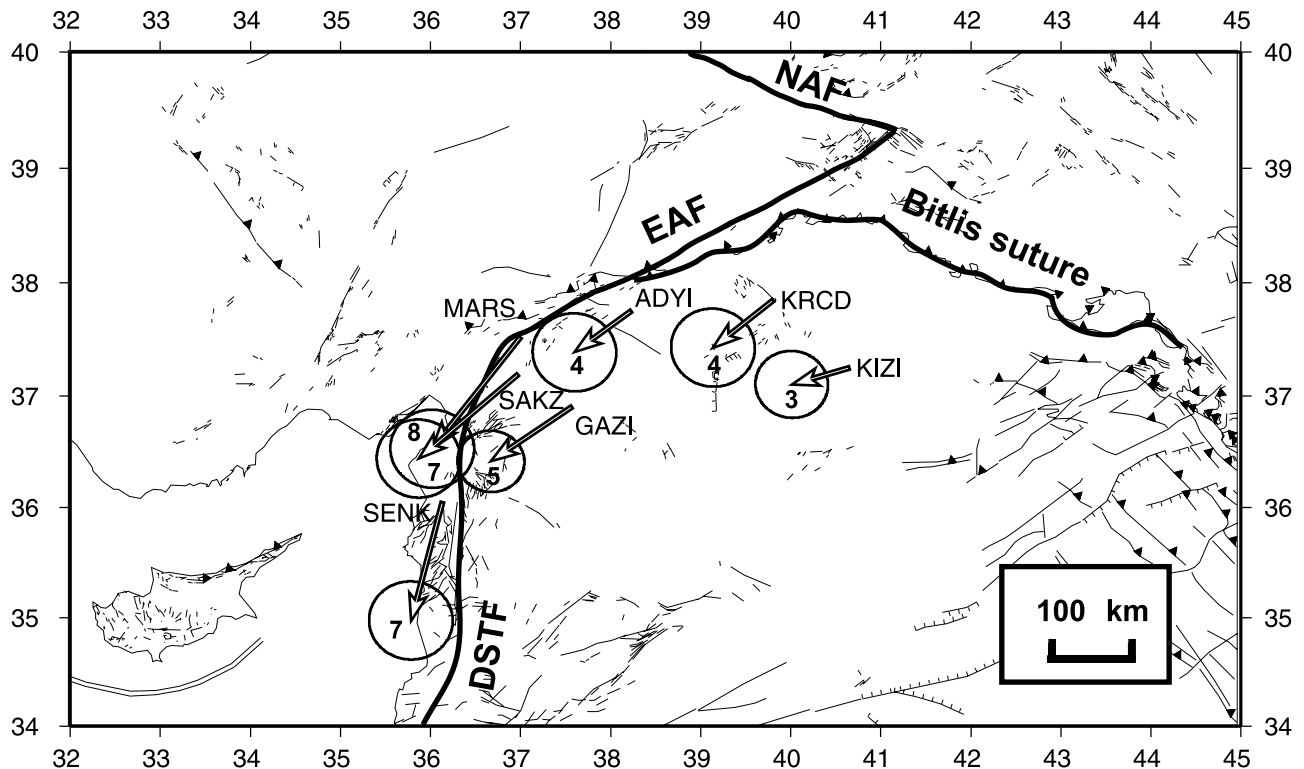


Figure 7. North Arabia site velocities from *McClusky et al.* [2000] rotated in our Arabian reference frame. Numbers next to arrow heads indicate the station velocity in mm/yr. Ellipses depict the 1σ uncertainties. Thick lines roughly depict faults in the area: East Anatolian Fault (EAF), North Anatolian Fault (NAF), Dead Sea Transform Fault (DSTF), and Bitlis suture zone.

rate compatible with the slowing down of Arabia [e.g., *Paul et al.*, 2001; *Sella et al.*, 2002; A. Socquet et al., unpublished manuscript, 2004]. However, when *Paul et al.*'s [2001] result is still too fast by 10%, *Sella et al.*'s [2002] relative pole predicts east-west compression on the plate boundary, in disagreement with observed strike-slip seismicity and transform fault azimuths. Using the angular velocity vector determined by A. Socquet et al. (unpublished manuscript, 2004) for India in the ITRF2000 (50.9°N , 12.13°W , $0.487^{\circ}/\text{Myr}$) (Table 2), we find an Arabia-India angular velocity (19.73°N , 20.42°E , $-0.035^{\circ}/\text{Myr}$) (Table 3). This predicts 2 mm/yr of strike-slip motion with an azimuth ranging from N-S in the north to $\text{N}15^{\circ}\text{E}$ in the south of the Owen fracture zone, in fair agreement with the direction of slip vectors in the area but with a reverse sense of motion: sinistral instead of dextral. In other words, the present-day geodetic determination of Indian and Arabian plates finds that India is still relatively faster than Arabia, when tectonic evidence from earthquakes fault plane solutions indicates the opposite. Mostly because they are small plates, finding a pole describing accurately the relative motion of India and Arabia with geodetic tools is a difficult task. In our solution, the residual motion of Bangalore (IISC) with respect to Arabia is very small: 0.9 mm/yr. This indicates that we roughly respect the close to zero relative motion between Arabia and India condition but cannot refine it further.

3.2.4. Arabia-Eurasia: Zagros Collision Zone

[22] A last test of our solution is the Arabia-Eurasia collision in Iran, where GPS data were made recently

available [*Nilforoushan et al.*, 2003; *Vernant et al.*, 2004]. We derived the Arabia-Eurasia rotation parameters (28.27°N , 12.12°E , $0.364^{\circ}/\text{Myr}$) from our solution for Arabia and from *Calais et al.*'s [2003] solution for Eurasia. Our pole is located far to the west of poles previously proposed on the basis of GPS data (Table 4). It is close to NUVEL-1A [*DeMets et al.*, 1994] pole, but the angular rate is reduced to $0.364^{\circ}/\text{Myr}$, much less than NUVEL-1A $0.520^{\circ}/\text{Myr}$. These parameters give a rate of convergence reduced to 21–27 mm/yr in the Zagros-Makran areas (instead of 32–38 mm/yr predicted by NUVEL-1A, a 30% reduction), consistent with the previous findings of *McClusky et al.* [2000], *Sella et al.* [2002], *Nilforoushan et al.* [2003], *McClusky et al.* [2003], and *Vernant et al.* [2004]. So again, we find a different rotation pole than previous studies because of new vectors in Yemen, but this different pole still predicts the same velocities as previous studies at stations in Bahrein and Oman.

[23] *McClusky et al.* [2000] used their own determination of Eurasia to define their reference frame. Because they do not give velocities in ITRF, direct comparison with our solution might be difficult. However, because the Eurasian determination of *Calais et al.* [2003] uses many common stations with *McClusky et al.* [2000], and in particular in Europe, the different frames should not generate discrepancies larger than 1–2 mm/yr, at least over our area of interest. In fact, we find exactly the same velocities (within <1 mm/yr) for stations NICO, NSSP, TRAB, and ZECK (Figure 3). Therefore we feel confident that we can “import” *McClusky et al.* [2000] velocities into our

reference frame without introducing significant distortion. Although it is around 150 km away from the East Anatolian Fault, station KIZI has a residual velocity of 3 mm/yr \pm 1.5 (Figure 7). Stations KRCD and GAZI are closer to the East Anatolian Fault (within 70 km) and have slightly higher residual velocities of 4 and 5 mm/yr, respectively. Finally, stations lying very close to the fault (MARS, SAKZ, SENK) show even higher residuals at 7–8 mm/yr (with the exception of ADYI which shows 4 mm/yr). Those residual velocities are not erratic but rather follow nicely the azimuth of the East Anatolian Fault (Figure 7). Also, although the numbers are small and one should be cautious because of GPS uncertainties, the decrease of residual velocity with the distance from the fault looks very much like the arctangent profile expected across a strike-slip fault locked at depth. Therefore we conclude that stations within 100 km from the East Anatolian Fault are affected by elastic deformation and should not be used to infer the rigid rotation parameters of the Arabian plate. On the opposite, they can be used to characterize the interseismic behavior of the fault and assess its locking depth. Given the far reach of the deformation (at least 100 km) and the slow rate on the fault (<10 mm/yr), this would imply a very large locking depth of at least 50 km, which seems unrealistic. Therefore we conclude that either our import of McClusky et al. data into our reference frame is not 100% correct and is affected by unconstrained reference frame rotations or there is widespread strain in addition to the elastic coupling. A fully comprehensive and more robust combination of the two data sets at the level of daily GPS observations is needed to further investigate this question.

4. Conclusion

[24] *Yang and Liu* [2002] have addressed the problem of the discrepancy between GPS data and NUVEL-1A at three convergent plate boundaries: the Andes, the Himalayas, and Taiwan. They concluded that the misfit can be explained by intraplate deformation. In the case of the Arabia-Eurasia convergence, such an explanation can be ruled out because we showed that the GPS rates of separation between Arabia and both Africa (in the Red Sea) and Somalia (in the Gulf of Aden) are reduced by 15–20% with respect to rates of spreading based on magnetic anomalies (and averaged over the last 3 Myr). We acknowledge the fact that differences in both rates and directions in the Red Sea are hardly significant and that this finding is better supported by Gulf of Aden data. Meanwhile, *Calais et al.* [2003] have shown that the Africa-Eurasia convergence rate has decreased since 3 Ma and rotated counterclockwise. We find, in agreement with former studies, that the rate of Arabia-Eurasia convergence has also decreased by \sim 30%, and we show that this is due not only to the decrease in the Africa-Eurasia convergence but also to a significant decrease in the separation rate between Arabia and Africa in the Red Sea (–15%) and Arabia and Somalia in the Gulf of Aden (–20%). We suggest that slow down of the Arabia-Eurasia convergence is due to decreasing of the slab pull force, resulting in reduced extension between Arabia and Africa-Somalia. Farther east, in the India-Eurasia convergence zone, GPS data also suggest a decrease in the convergence

rate [*Paul et al.*, 2001; *Wang et al.*, 2001; A. Socquet et al., unpublished manuscript, 2004]. With our definition of Eurasia, which follows that of *Calais et al.* [2003], and the rotation of India from A. Socquet et al. (unpublished manuscript, 2004), we also find a lower India-Eurasia collision rate than NUVEL-1A. This discrepancy is due to either an overestimation of the rate in NUVEL-1A or to an actual slowing down of the Indian plate. If the second possibility is confirmed, then it would appear that the whole collision zone between Africa, Arabia, India and Eurasia has slowed down in the last 3 Myr.

[25] **Acknowledgments.** We thank the many people, too numerous to be all cited, involved in the acquisition of the GPS data from 1991 to 2001: especially the IT-Iran group (represented by D. Hatzfeld) for their recent measurements in Oman and Iran, P. Briole for sharing his data on La Réunion, the Yemen Survey Authority and the University of Sana'a for their support in Yemen, and A. Abdallah (ISERST) and all people at "Observatoire d'Arta" in the Republic of Djibouti for their continuous efforts. Financial support for both the field work and the data analysis was provided by the French INSU/CNRS (programmes AFAR, Tectoscope-positionnement, PNTS, IT-Iran, IT-Panaches) and the French Embassy in the Republic of Yemen.

References

- Altamimi, Z., P. Sillard, and C. Boucher (2002), ITRF2000: A new release of the International Terrestrial Reference Frame for earth science applications, *J. Geophys. Res.*, *107*(B10), 2214, doi:10.1029/2001JB000561.
- Argus, D. F., and R. G. Gordon (1991), No-net-rotation model of current plate velocities incorporating plate motion model NUVEL-1, *Geophys. Res. Lett.*, *18*, 2039–2042.
- Banerjee, P., and R. Bürgmann (2002), Convergence across the northwest Himalaya from GPS measurements, *Geophys. Res. Lett.*, *29*(13), 1652, doi:10.1029/2002GL015184.
- Beutler, G., J. Kouba, and T. Springer (1993), Combining the orbits of the IGS processing centers, in *Proceedings of IGS Analysis Center Workshop*, edited by J. Kouba, pp. 20–56, Geod. Surv. Div., Nat. Resour. Can., Ottawa, Canada.
- Bilham, R., R. Bendick, K. Larson, P. Mohr, J. Braun, S. Tesfaye, and L. Asfaw (1999), Secular and tidal strain across the Main Ethiopian Rift, *Geophys. Res. Lett.*, *26*, 2789–2792.
- Calais, E., C. DeMets, and J.-M. Nocquet (2003), Evidence for a post-3.16–Ma change in Nubia-Eurasia-North America plate motions?, *Earth Planet. Sci. Lett.*, *216*, 81–92.
- Chu, D., and R. G. Gordon (1998), Current plate motions across the Red Sea, *Geophys. J. Int.*, *135*, 313–328.
- Chu, D., and R. G. Gordon (1999), Evidence for motion between Nubia and Somalia along the southwest Indian Ridge, *Nature*, *398*, 64–67.
- DeMets, C., R. G. Gordon, D. Argus, and S. Stein (1994), Effect of recent revisions to the geomagnetic reversal time scale on estimates of current plate motions, *Geophys. Res. Lett.*, *21*, 2191–2194.
- Dewey, J. F., M. L. Helman, E. Turco, D. H. W. Hutton, and S. D. Knott (1989), Kinematics of the western Mediterranean, in *Alpine Tectonics*, edited by M. P. Coward, D. Dietrich, R. G. Park, *Geol. Soc. Spec. Publ.*, *45*, 265–283.
- Fernandes, R. M. S., B. A. C. Ambrosius, R. Noomen, L. Bastos, M. J. R. Wortel, W. Spakman, and R. Govers (2003), The relative motion between Africa and Eurasia as derived from ITRF2000 and GPS data, *Geophys. Res. Lett.*, *30*(16), 1828, doi:10.1029/2003GL017089.
- Herring, T. A. (1999), Documentation for the GLOBK software version 5.01, Mass. Inst. of Technol., Cambridge.
- Herring, T. A., J. L. Davis, and I. I. Shapiro (1990), Geodesy by radio interferometry: The application of Kalman filtering to the analysis of very long baseline interferometry data, *J. Geophys. Res.*, *95*, 12,561–12,581.
- Jestin, F., P. Huchon, and J. M. Gaulier (1994), The Somalia plate and the East African Rift system: Present day kinematics, *Geophys. J. Int.*, *116*, 637–654.
- King, R. W., and Y. Bock (2000), Documentation for the GAMIT GPS software analysis version 9.9, Mass. Inst. of Technol., Cambridge.
- Klinger, Y., J. P. Avouac, N. Abou Karaki, L. Dorbath, D. Bourles, and J. L. Reyss (2000), Slip rate on the Dead Sea transform fault in northern Arabia valley (Jordan), *Geophys. J. Int.*, *142*, 755–768.
- Kreemer, C., W. E. Holt, and J. Haines (2003), An integrated global model of present-day plate motions and plate boundary deformation, *Geophys. J. Int.*, *154*, 1–27.

- Larson, K. M., J. T. Freymueller, and S. Philipson (1997), Global plate velocities from the Global Positioning System, *J. Geophys. Res.*, *102*, 9961–9981.
- McClusky, S., et al. (2000), Global Positioning System constraints on plate kinematics and dynamics in the eastern Mediterranean and Caucasus, *J. Geophys. Res.*, *105*, 5695–5720.
- McClusky, S., R. Reilinger, S. Mahmoud, D. Ben Sari, and A. Tealeb (2003), GPS constraints on Africa (Nubia) and Arabia plate motions, *Geophys. J. Int.*, *155*, 126–138.
- Neilan, R. (1995), The evolution of the IGS global network, current status, and future aspects, in 1995 IGS Annual Report, edited by J. F. Zumberge et al., *JPL Publ.*, 95-18, 25–34.
- Nilforoushan, F., et al. (2003), GPS network monitors the Arabia-Eurasia collision deformation in Iran, *J. Geod.*, *77*, 422–441.
- Nocquet, J. M., E. Calais, Z. Altamimi, P. Sillard, and C. Boucher (2001), Intraplate deformation in western Europe deduced from an analysis of the ITRF97 velocity field, *J. Geophys. Res.*, *106*, 1239–1258.
- Patriat, P., and J. Achache (1984), India Eurasia collision chronology has implications for crustal shortening and driving mechanism of plates, *Nature*, *311*, 615–621.
- Paul, J., et al. (2001), The motion and active deformation of India, *Geophys. Res. Lett.*, *28*, 647–650.
- Pe'eri, S., S. Wdowinski, A. Shtibelman, N. Bechor, Y. Bock, R. Nikolaidis, and M. van Domselaar (2002), Current plate motion across the Dead Sea Fault from three years of continuous GPS monitoring, *Geophys. Res. Lett.*, *29*(14), 1697, doi:10.1029/2001GL013879.
- Prawirodirdjo, L., and Y. Bock (2004), Instantaneous global plate motion model from 12 years of continuous GPS observations, *J. Geophys. Res.*, *109*, B08405, doi:10.1029/2003JB002944.
- Quittmeyer, R. C., and A. L. Kafka (1984), Constraints on plate motions in southern Pakistan and the northern Arabian Sea from the focal mechanisms of small earthquakes, *J. Geophys. Res.*, *89*, 2444–2458.
- Rosenbaum, G., G. S. Lister, and C. Duboz (2002), Relative motions of Africa, Iberia and Europe during alpine orogeny, *Tectonophysics*, *359*, 117–129.
- Ruegg, J. C., et al. (1993), First epoch geodetic GPS measurements across the Afar Plate boundary zone, *Geophys. Res. Lett.*, *20*, 1899–1902.
- Sella, G. F., T. H. Dixon, and A. Mao (2002), REVEL: A model for Recent plate velocities from space geodesy, *J. Geophys. Res.*, *107*(B4), 2081, doi:10.1029/2000JB000033.
- Tamsett, D., and R. Searle (1988), Structure and development of the midocean ridge plate boundary in the Gulf of Aden: Evidence from GLORIA side scan sonar, *J. Geophys. Res.*, *93*, 3157–3178.
- Vernant, P., et al. (2004), Contemporary crustal deformation and plate kinematics in Middle East constrained by GPS measurements in Iran and northern Oman, *Geophys. J. Int.*, *157*, 381–398, doi:10.1111/j.1365-246x.2004.02222.x.
- Walpersdorf, A., C. Vigny, J.-C. Ruegg, P. Huchon, L. M. Asfaw, and S. Al Kirbashi (1999), 5 years of GPS observations in the Afar Triple Junction area, *J. Geodyn.*, *28*(2–3), 225–236.
- Wang, Q., et al. (2001), Present-day crustal deformation in China constrained by Global Positioning System measurements, *Science*, *294*, 574–577.
- Wdowinski, S., Y. Bock, G. Baer, L. Prawirodirdjo, N. Bechor, S. Naaman, R. Knafo, Y. Forrai, and Y. Melzer (2004), GPS measurements of current crustal movements along the Dead Sea Fault, *J. Geophys. Res.*, *109*, B05403, doi:10.1029/2003JB002640.
- Williams, S. D. P., Y. Bock, P. Fang, P. Jamason, R. M. Nikolaidis, L. Prawirodirdjo, M. Miller, and D. J. Johnson (2004), Error analysis of continuous GPS position time series, *J. Geophys. Res.*, *109*, B03412, doi:10.1029/2003JB002741.
- Yang, Y., and M. Liu (2002), Deformation of convergent plates: Evidence from discrepancies between GPS velocities and rigid-plate motions, *Geophys. Res. Lett.*, *29*(10), 1472, doi:10.1029/2001GL013391.

L. M. Asfaw, Department of Geophysics, Addis Ababa University, P.O. Box 1176, Addis Ababa, Ethiopia.

P. Huchon and C. Vigny, Laboratoire de Géologie, Ecole Normale Supérieure, CNRS, 24 rue Lhomond, F-75231 Paris cedex 05, France. (philippe.huchon@lgs.jussieu.fr; vigny@geologie.ens.fr)

K. Khanbari, Department of Geosciences, Sana'a University, P.O. Box 14433, Sana'a, Yemen. (kkhanbari@hotmail.com)

J.-C. Ruegg, Laboratoire de Sismotectonique, IPGP, 4 place Jussieu, F-75005 Paris, France. (ruegg@ipgp.jussieu.fr)